Thermal performance evaluation and energy saving potential of semi-transparent CdTe in Façade BIPV

ALRASHIDI, Hameed, ISSA, Walid <http://orcid.org/0000-0001-9450-5197>, SELLAMI, Nazmi, SUNDARAM, Senthilarasu and MALLICK, Tapas

Thermal Performance Evaluation and Energy Saving Potential of Semi-transparent CdTe in Façade BIPV

Abstract

Semi-transparent PV glazing are promising in Building Integrated Photovoltaic (BIPV) applications. They provide daylight control, energy saving and power generation. The selection of optimal Photovoltaic (PV) glazing requires the accounting for various factors such as location, orientation and glazing transparency. In this work, thermal performance of Cadmium telluride (CdTe) based semi-transparent PV glazing of different transparencies was evaluated in UK for South and South-West orientations. Thermal performance was analysed in terms of U-value, SHGC and cooling load. Results revealed that least transparency CdTe PV glazing can have U-values as low as 1.52 W/m²K. The use of least transparency PV glazing can reduce 96% of solar heat gains and 23.2% of cooling energy compared to conventional clear glazing when used in South-West orientation. The selection of optimum glazing was discussed taking into consideration occupants' optical comfort and health.

Nomenclature

A_i	Anisotropy index
$I_{beam,h}$	Incident beam solar radiation on the horizontal surface
$I_{diff,h}$	Incident diffuse solar radiation on the horizontal surface
I_{global}	Incident global solar radiation
M_{tc}	Mass of the air inside the test cell
Q_{in}	Total power incident on gazing
Q_{loss}	Heat loss through the walls of the test cell
Q_{tc}	Total power stored inside the test cell
$SHGC$	Solar Heat Gain Coefficient
T	temperature
t	time
$T_{tc,in}$	Temperature inside the test cell
$T_{tc,out}$	Ambient temperature
TSE	Transmitted Solar Energy
U_g	overall heat transfer coefficient of glazing
β	Glazing tilt angle
τ	transmittance
τ_v	Vertical global transmittance
τ_{dir}	direct transmittance
τ_{dif}	Diffuse transmittance

1. Introduction

The use of glazing as exterior building facades provide daylight, good ambience to the occupants, more interaction with outdoor environment and an enhanced aesthetic view for the building. However, the heat gains or losses through the glazing facades play a key role in determining cooling and heating loads. Glazing allows the transmission of a high amount of heat because of their high

overall heat transfer coefficients "U-values" (*Fenestration of Today and Tomorrow: A State-of-the-Art Review and Future Research Opportunities*, 2012). This encourages new glazing technologies with low U-values to be developed to allow for more energy savings and boost the efficiency of the future buildings.

In order to control the heat gains or losses, switchable transparency glazing and constant transparency glazing were developed as presented. Switchable transparency glazing can alter their optical transmission (a) electrically through an external source or (b) non-electrically (Ghosh et al., 2016) (Allen et al., 2017)(Rezaei et al., 2017). As for constant transparency glazing, they are of different types including aerogel vacuum (Schultz & Jensen, 2008), low e-coating (Somasundaram et al., 2020) , and semi-transparent PV glazing. Fixed shading devices can be added to constant transparency glazing in order to reduce the solar radiation subjected to windows (Favoino et al., 2016)(Alzoubi & Al-Zoubi, 2010). However, these devices block the beneficial winter solar radiation and reduce the daylight availability which leads to an increasing need of artificial lighting (Bellia et al., 2013)(Mandalaki et al., 2012).

PV glazing can be of different transparencies and it is the only glazing technology that generates electricity (Samir & Ali, 2017)(N. Skandalos & Karamanis, 2016)(Liao & Xu, 2015). A promising application of constant transparency glazing is the semi-transparent PV glazing as BIPV (Khalifeeh et al., 2021). Among the different types of PV glazing, thin-film PV; that includes amorphous silicon (Wang et al., 2017) (Song et al., 2008), CIGS (Sidali et al., 2018) (Alaaeddin et al., 2019), CdTe (Alrashidi, Issa, et al., 2020); are favored in BIPV applications as they are advantageous in terms of availability of raw materials, having light weight, having aesthetic appearance and having high transparency levels while keeping acceptable efficiencies (Nikolaos Skandalos & Karamanis, 2015)(Biyik et al., 2017)(Meillaud et al., 2015). The performance of a thin-film based PV glazing is affected by various factors. In Madrid, Olivieri et al. (Olivieri et al., 2014) investigated four amorphous silicon semi-transparent thin-film PV modules of different transmittances. The study found that the solar protection and insulating properties of amorphous-silicon PV modules are lower than those achieved by a reference glazing. Fung et al. (Fung & Yang, 2008) developed a semi-transparent PV heat gain model. Their experiment was conducted on poly-crystalline Edge-defined Film-fed Growth (EFG) silicon semi-transparent module. Their results emphasized the effect of solar cell area on the total heat gain passing through the glazing. Evaluation of optical and thermal properties of semi-transparent amorphous silicon (a-Si: H) solar cells in various conditions revealed that a significant effect on energy saving was noticed by changing the thermo-optical characteristics of the glazing (Chae et al., 2014). Another study by Peng et al. showed that the use of correct ventilation mode enhances the energy saving and PV power generation of double-skin amorphous silicon (a-Si) PV (Peng et al., 2015). In another work, the effect of location on PV cell performance was investigated by comparing the optimum performance of PV window when applied in London and Madrid. The authors illustrated the difference in performance by the amount of daylight that reaches the glazing in each city (Yun et al., 2007). A study in tropical Singapore climate revealed that the solar heat gain of a semi-transparent PV glazing is dependent on the orientation of the module (Chen et al., 2012). Altering the orientation of PV module, represented by azimuth angle, and shading factors provided a significant improvement for PV energy generation by 47% in Korea (Yoon et al., 2011).

CdTe is a promising type of thin-film PV, due to its cost-effectiveness, high efficiency (Noufi & Zweibel, 2006)(Romeo et al., 2014) and direct optical bandgap (1.45 eV) that matches with solar spectrum for PV energy conversion (McCandless & Sites, 2011). In India's composite climate, a numerical investigation on energy saving potential of semi-transparent CdTe PV prevailed that maximum energy saving can be achieved by deploying lowest transparency module in South direction. The authors emphasized the effect of orientation and PV transparency on energy performance and encouraged focus on these variables (Barman et al., 2018). The energy and optical performance of 10% transparent double-skin CdTe PV glazing was studied numerically (Sun et al., 2018). They pointed out that for high window-to-wall ratio (>45%) a 73% energy saving can be achieved compared to conventional double glazing. Also, the CdTe PV glazing was advantageous over conventional double glazing by reducing the interior daylight glare. Thermal performance of CdTe PV window in temperate climate was studied by (Alrashidi, Ghosh, et al., 2020). The use of 25% visible transmission and 12% solar transmission CdTe glazing could provide 37% lower heat loss than conventional single glazing.

Based on the above discussion, different variables affect the performance of a PV glazing including the type and transparency of PV module as well as the location and orientation of deployment. This paper presents the first outdoor experimental thermal performance characterization of CdTe PV non-ventilated glazing as BIPV façade in the UK while taking into consideration the effect of façade orientation and optical parameters. Thermal performance was evaluated through U-values, solar heat gains and cooling load. Results are compared to conventional single glazing for clear assessment of energy saving potential. The selection of optimum PV transparency was discussed in light of different factors.

2. Experimental Setup

2.1 Outdoor Experiment

Eight test cells were installed in two different orientations, namely South and South-West, at Penryn, UK where latitude and longitude coordinates are 50.169174 and -5.107088 respectively. The South and South West orientations were particularly taken into consideration since they are the most favorable for PV applications (Somasundaram et al., 2020). Each test cell was fitted with one glazing in such a way that the performance of three different CdTe PV glazing (S_1, S_2 and S_3) can be tested in both orientations in comparison to single glazing (S_0), considering the window-to-wall ratio as 100%. The samples S_0 to S_3 parameters are shown in table 1. Test cells sizes are (0.22 m x 0.2 m x 0.18 m), and are made of polyisocyanurate insulation board (thickness 2.5cm, thermal conductivity 0.02 W/mK) to provide good insulation so that one dimensional heat transfer through the glazing can be assumed. Peltier-based air conditioning (AC) units were fitted to each test cell to be used as cooling unit run by a temperature regulator. However, it might be turned off completely in selected days for thermal performance evaluation.

Table 1 Glazing specifications

Parameter	S0	S1	S2	S3
Transparency	90%	24.83%	18.66%	0.46%
Output power	Ø	0.815 Wp	0.996 Wp	1.414 Wp

K-type thermocouples were used to monitor the temperatures inside the test cells and at the inner and outer surfaces of each glazing. Data acquisition and logging was implemented using Arduino microcontroller for South-West oriented test cells and Omega microcontroller for South oriented test cells. Pyranometer and pyrheliometer were used to measure direct, global and diffuse solar irradiances. Figures 1and 2 show a photograph and a sketch of the experimental setup respectively.

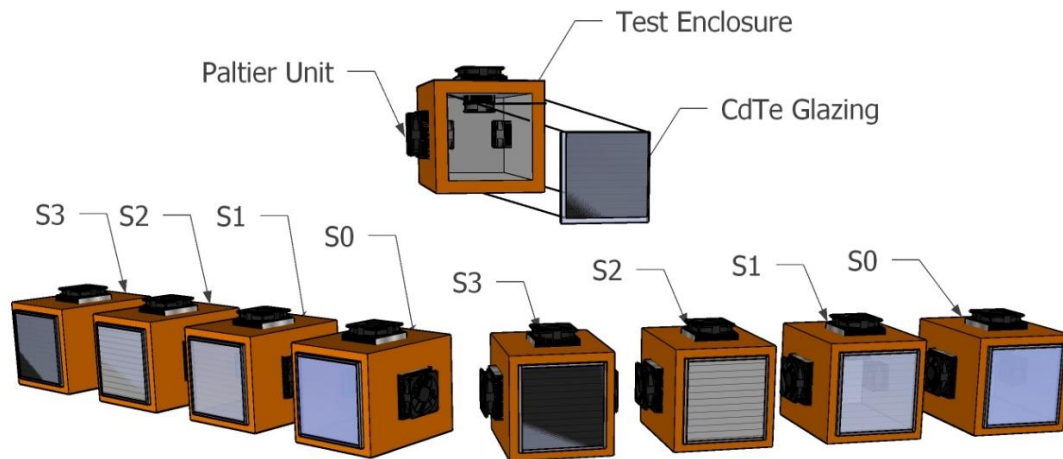Figure 1. A labelled photograph of the outdoor experimental setup showing the eight test cells

Figure 2. Sketch of the outdoor experimental setup showing the eight test cells – The outer shield box was omitted for clarity

Throughout data gathering, cloudy days, intermittent cloudy days and sunny days were observed. Thermal parameters are affected by solar irradiance, ambient temperature and wind speed. Cloudy and intermittent cloudy days would result in higher ambient conditions fluctuation. Therefore, a sunny day, on 25th of September, was selected for thermal performance analysis to get the highest possible rate of heat transfer and steadiest ambient conditions so that an average value of a lengthy experiment can give the closest figure of a steady state condition. Figure 3 exhibits the direct vertical solar irradiance and power generated by each PV glazing in South and South-West

orientation. S3 was found to benefit the most from solar irradiance generating more maximum power than S2 and S1 by 146% and 133% respectively in South-West direction and 153% and 137% in South orientation. Both orientations show close values, the difference in PV power generation can be due to difference in direct solar irradiance, PV cells operating temperature (Amelia et al., 2016) and soiling factors (Smestad et al., 2020). However, during the test period, the test cells were cleaned, and the soiling impact has been mitigated.
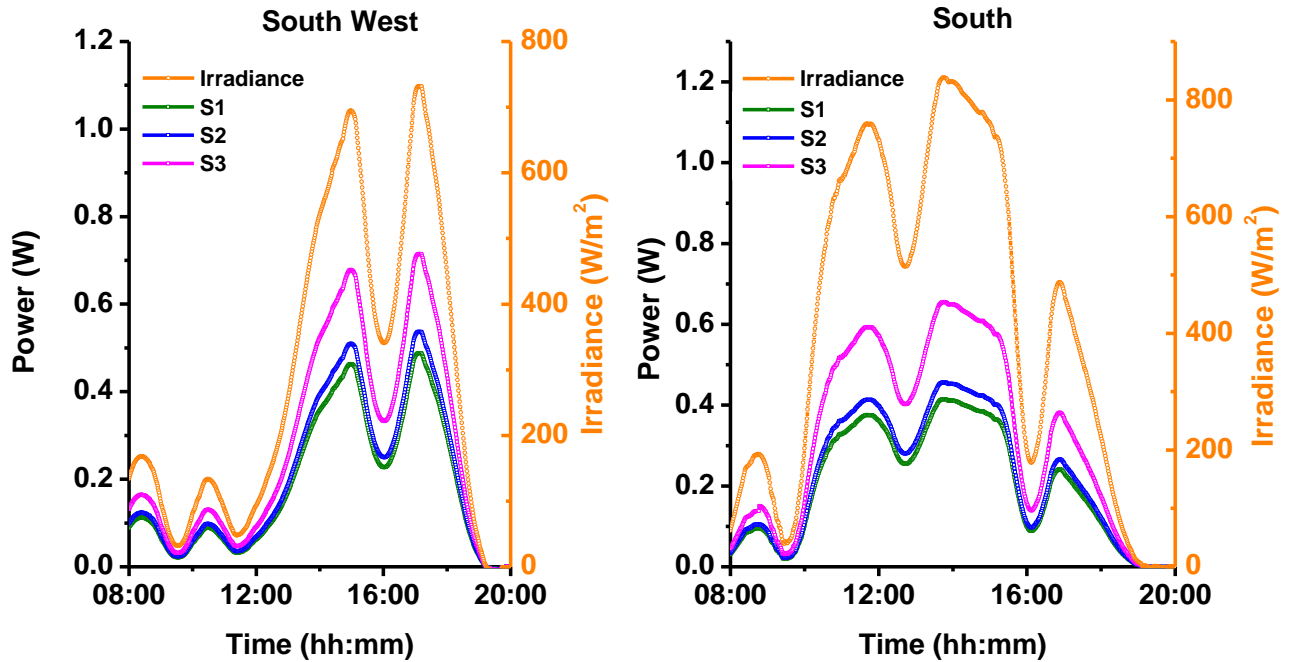

Figure 3. Diurnal variation of power and solar irradiance in South and South-West orientations on 25th of September

2.2 Indoor Experiment

Indoors, a constant irradiance solar simulator (Class AAA+, AM 1.5) and a 1.5 m/s constant speed fan were used to emulate the outdoor solar irradiance and wind speed respectively. The solar simulator provided 300 W/m^2 constant irradiance that is equivalent to the average solar irradiance outdoor. The experiment was conducted for eight continuous hours for each test cell so that steady state heat transfer can be achieved and then a proper thermal assessment can be obtained. Figure 4 shows a photograph of the indoor experiment.
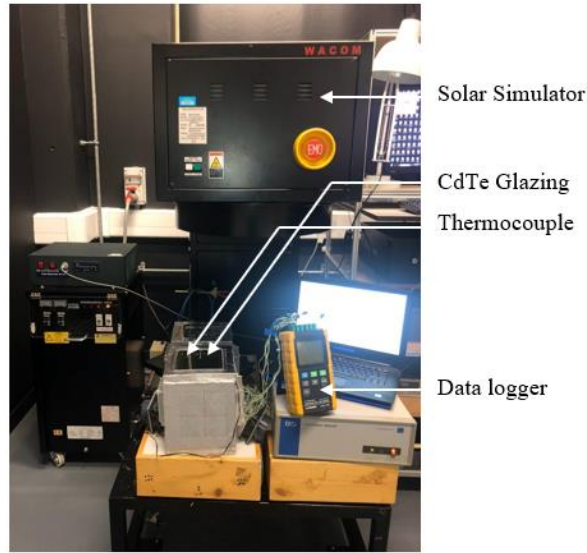
Figure 4. Photograph of the indoor experiment

Indoor spectral measurements were performed to obtain the optical transmittances of the glazing under study using Perkin Elmer Lambda 1050 spectrometer. Figure 5 shows that the visible transmittance of S1, S2 and S3 are 24.83%, 18.66% and 0.46% respectively, less than that of clear single glazing whose transmittance was found to be 90%.
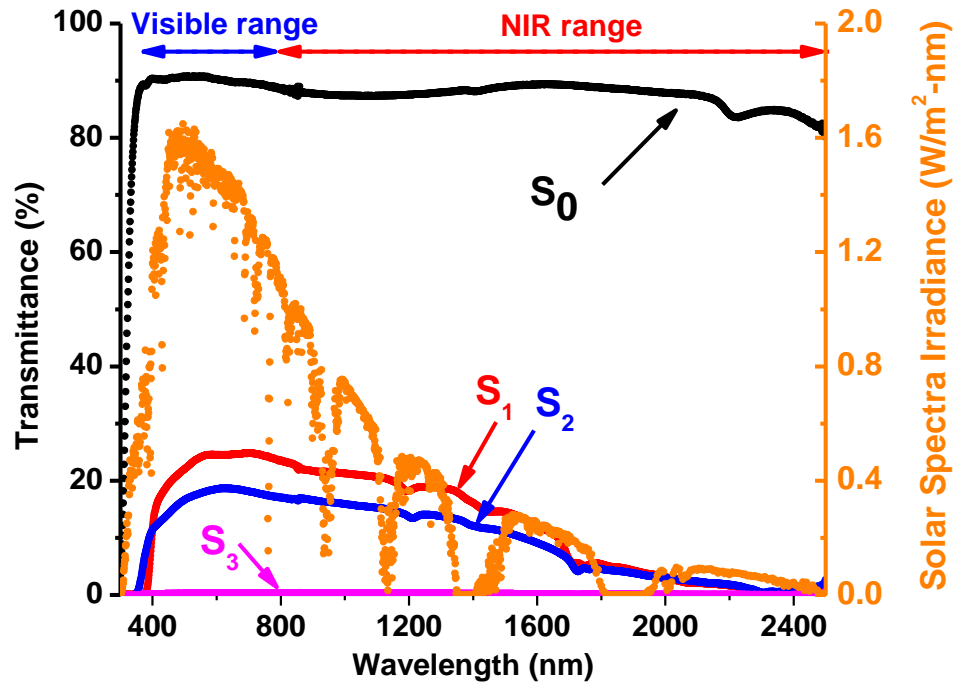

Figure 5. Spectral irradiance and solar transmittance of Semi-Transparent (STPV) glazing and single glazing in visible transmittance range (380-780nm) and NIR transmittance range (780-2500nm)

3. Thermo-optical Performance

Figures 6 shows the diurnal variation of test cell and inner surface temperatures obtained from outdoor experiment in both South and South-West orientations. Results show that single glazing S_0 recorded the highest interior temperature. Whereas for PV cells S_1, S_2 and S_3, higher transparency glazing record higher test cell temperature. This behaviour was noticed in both orientations with South orientation having higher temperatures prior to midday and South West orientation having higher temperature post midday due to sun trajectory. A reverse behaviour was registered for inner surface temperatures as lower transparency glazing recorded higher Temperatures. This can be referred to the fact that semi-transparent PV glazing absorbs solar radiation in order to generate electric power. The surface temperature of PV glazing in South orientation was found to be lower than that of South-West orientation at peak temperature time, this justifies the higher power generation that was registered for South orientation in figure 2, as lower PV operating temperatures result in higher PV cell efficiency. Very similar variations in test cell and inner surface temperatures were achieved in the indoor experiment as shown in figure 7. It was observed that the temperatures of the solar cells' surfaces and the indoor temperatures of the test cells reached steady-state values after 8 hours of continuous testing in indoor conditions.
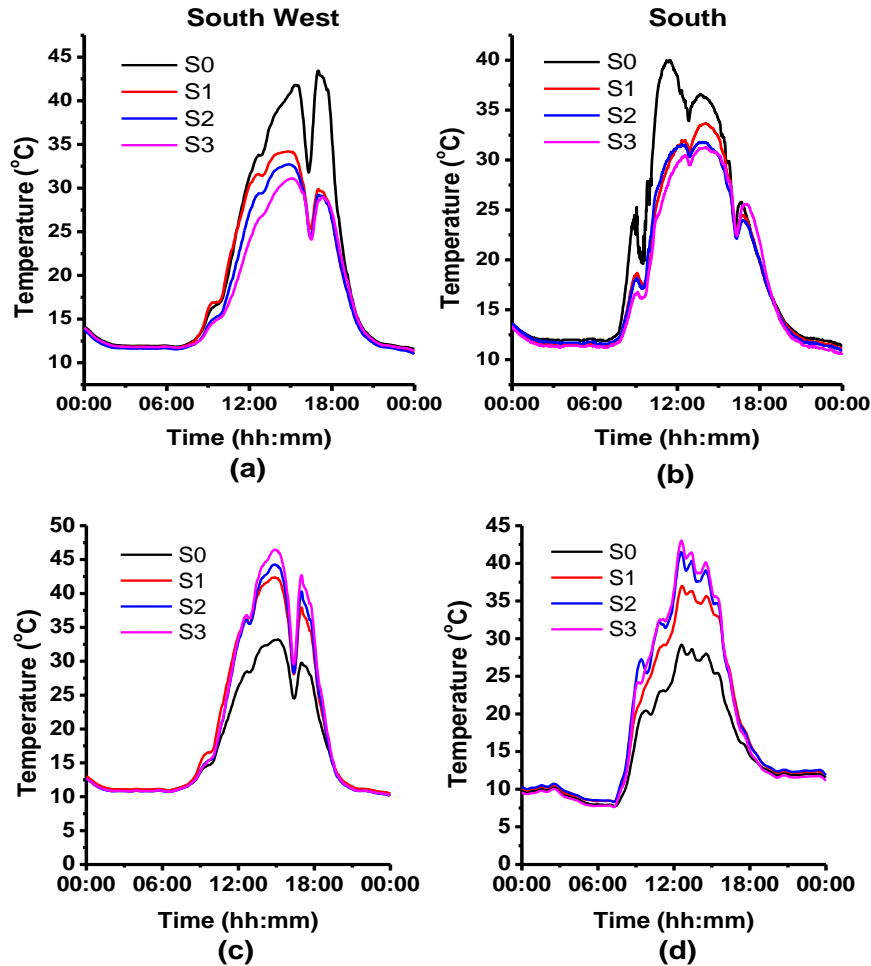

Figure 6. Diurnal variation of all test cells inside temperatures (a) and (b) and inner surface temperatures (c) and (d) on 25th of September
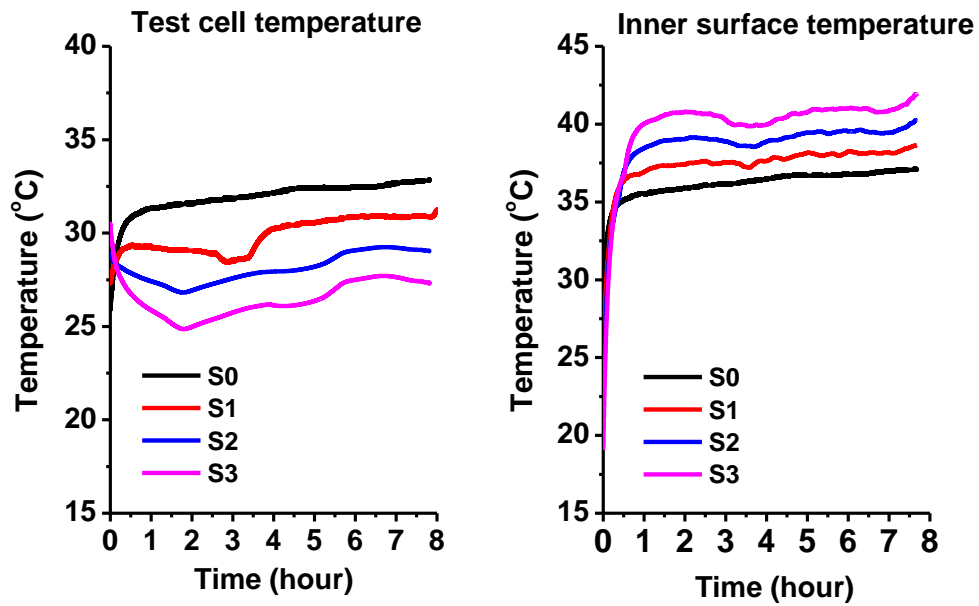
7

Figure 7. Diurnal variation of test cell indoor temperature and inner surface temperature in indoor experiment

Figure 7 shows how each transparency impacts the indoor temperature of the Test cell. Clearly, it is illustrated that the opaquer solar cell maintains lower indoor temperature than more transparent ones. However, the inner surface of the opaquer solar cell is the highest. The reverse behavior between the interior and inner surface temperatures can be illustrated by the absorption response of all samples. Figure 8 shows the absorbance curves over the wavelength range. The lower transparency glazing, S3, resulted in a higher overall absorbance in the visible and NIR ranges, which is converted to heat relatively higher than other samples. Another factor is how the active material is sandwiched between two panes, as there is no distances or insulation gas to reduce the outer to inner surfaces conduction. The accumulation of absorbed solar radiation causes an increase in the surface temperature of the glazing.

For the most transparent cell, it will trap more heat inside the room relatively higher than other samples and due to the capacity of the room, it impacts the inner surface to keep it within its vicinity.
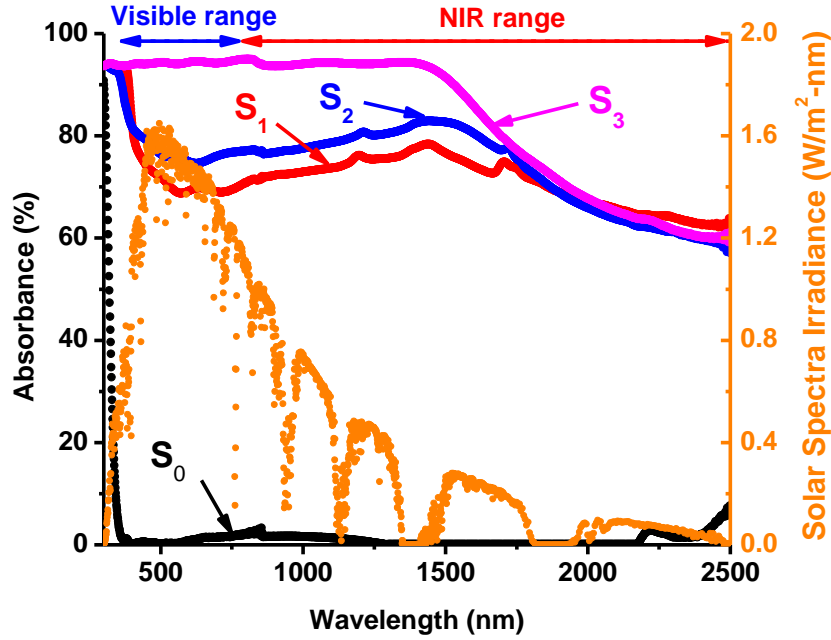
8

Figure 8. Spectral irradiance and absorbance of STPV glazing and single glazing in visible transmittance range (380-780nm) and NIR transmittance range (780-2500nm)

4. Thermal Performance

4.1 Solar heat gain coefficient

Solar heat gain coefficient (SHGC) measures the fraction of global irradiance that is transmitted through the glazing. SHGC of each glazing was calculated using equation (1) (Alrashidi, Ghosh, et al., 2020)

$$SHGC = \frac{TSE}{I_{ver,global}} \tag{1}$$

Where; TSE is the transmitted solar energy and it can be evaluated as in equation (2).

$$TSE = \left(I_{beam,h} + I_{dif,h}A_i\right)\tau_{dir}r_b + I_{dif,h}\left(1+A_i\right)\tau_{dif,h}\frac{\left(1+\cos\beta\right)}{2} + I_{global}\rho_g\tau_g\frac{\left(1-\cos\beta\right)}{2} \tag{2}$$

SHGC is associated with direct, diffused and reflected solar radiation, therefore it is dependent on the incident angle (Waide & Norton, 2003). Figure 9 shows the variation of outdoor solar heat gain coefficients with incident angle for South and South-West orientations. Results reveal that the maximum reduction in solar gain for Semi-Transparent (STPV) glazing S_1, S_2 and S_3 are 72.3%, 80%, and 96% respectively compared to single glazing S_0 as a reference. Results of SHGC signify that for hot climates, the use of semi-transparent PV glazing is favourable for limiting solar heat gains and reducing cooling loads. The maximum SHGC of single glazing was found to be 71.3%, this agrees with the values of NFRC (Efficientwindows, 2018). Close SHGCs were found in both tested orientations with slightly higher values registered for South orientation.

9

Also, it was observed that the variation of the angles of incidence from 0 degrees to 50 degrees doesn't affect the variation of the SHGC values. They remain constant from 0 degrees to 55 degrees where they started dropping to reach zero value for an angle of incidence equal to 90 degrees. (Sunrays parallel to the tested glazing cells)
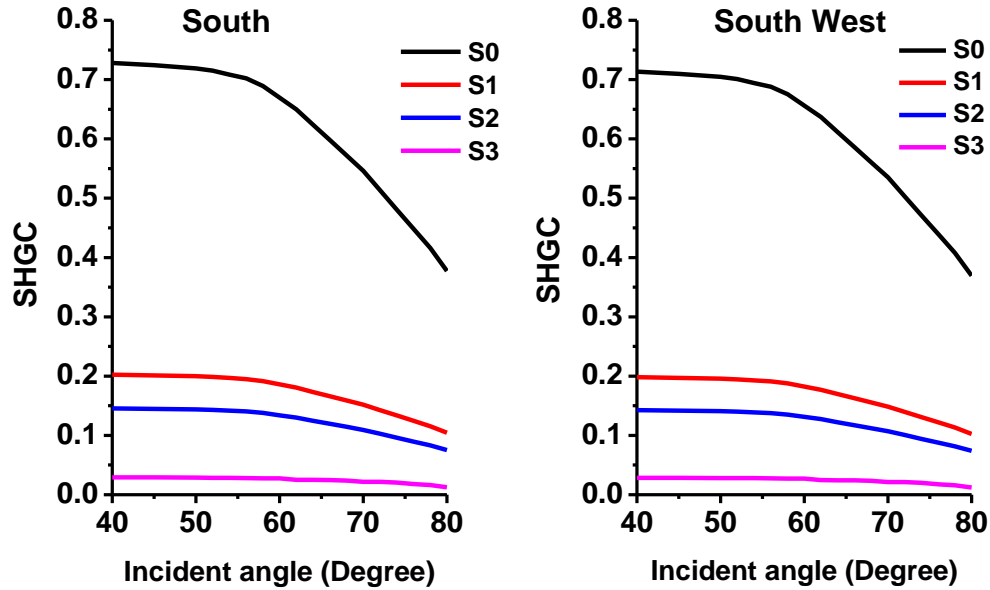

Figure 9. Variation of SHGC with incident angle in South and South West Directions

4.2 Overall heat transfer coefficient

The overall heat transfer coefficient (U-value) measures how well a glazing conducts heat through radiation, conduction and convection. Equation (3) was used to calculate the U-value under the assumptions of one dimensional steady state heat transfer and zero ground solar radiation reflection. (Alrashidi, Ghosh, et al., 2020)

$$U_g = \frac{Q_{in} - Q_{tc} - Q_{loss} - P_g}{A_g (T_{tc,in} - T_{tc,out})} \tag{3}$$

Where

Aperture area of glazing (A_g) is 0.0225 m^2

$$Q_{in} = I(t) A_g \tau_v(\theta) \alpha \tag{4}$$

$$Q_{tc} = M_{tc} C_{tc} \frac{dT}{dt} \tag{5}$$

Where mass of air inside the test cell (M_{tc}) and its heat capacity (C_{tc}) are 0.08 kg and 1.006 kJ/kgK respectively.

$$Q_{loss} = Q_{wall} = (UA)_{wall}(T_{tc,in} - T_{tc,out})$$ (6)

Figure 10 exhibits the diurnal variation of U-values of S_0, S_1, S_2 and S_3 in South and South West orientations. U-values show a fluctuating behavior throughout the day, this is due to the dynamic ambient conditions of solar irradiance, wind speed and ambient temperature. However, an average value can be considered since the experiment is carried out for a long period of time. In South orientation, the average calculated U-values were 5.6, 2.64, 2.35 and 1.54, while in South West, average U-values were 5.67, 2.7, 2.33 and 1.52 for S0, S1, S2 and S3 respectively. Similar results were obtained from the indoor experiment in figure 11, as the U-values of S_0, S_1, S_2 and S_3 were found to be 5.7, 2.7, 2.3 and 1.52 respectively. Indoor experiment has shown steadier results than outdoor because of the constant irradiance from the solar simulator, constant indoor ambient temperature and constant wind speed from the constant speed fan.

Low U-value of glazing is always required to maintain the achieved temperature difference between the interior of the room and the ambient thus saving energy required for heating and cooling. Cold climates favors glazing with high SHGC to benefit from maximum solar heat gains and minimize the energy consumption for heating loads, whereas low SHGC glazing are required for hot and warm climates to reduce cooling load requirements. The quantification of thermal properties emphasizes the use of the studied PV glazing in hot climates.
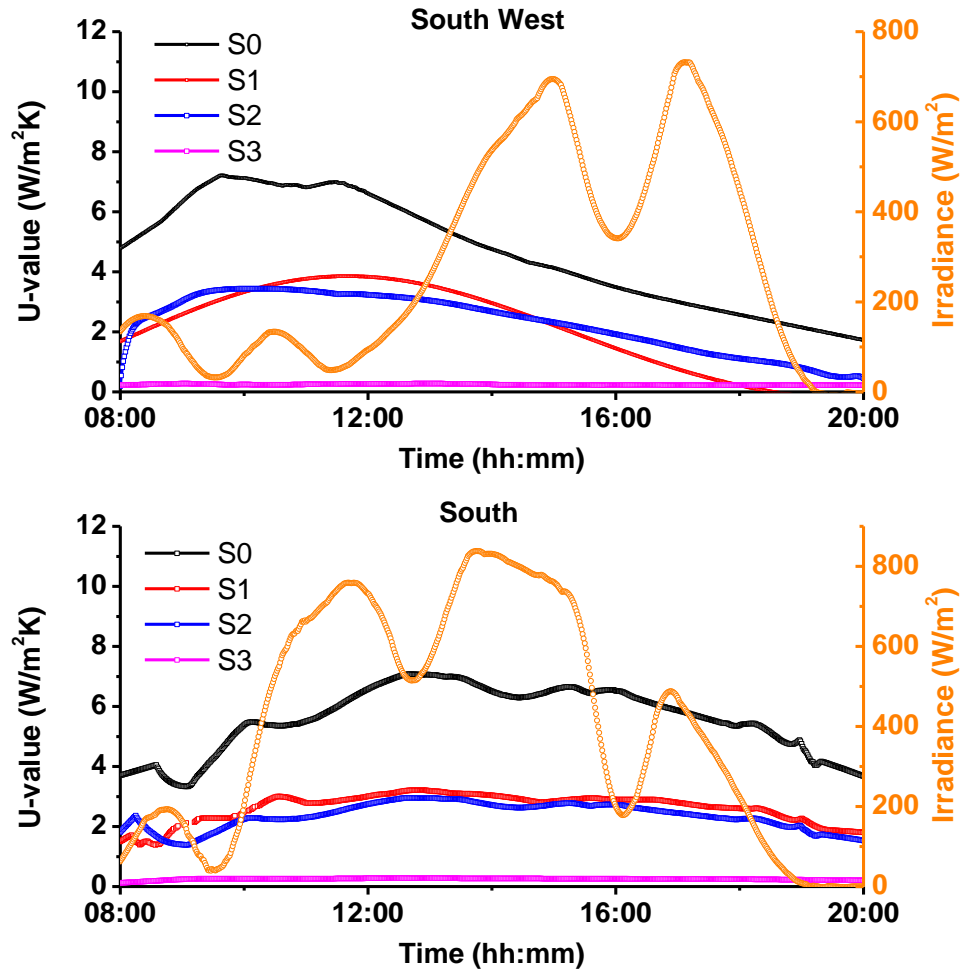
Figure 10. Diurnal variation of U-values and ambient temperature in outdoor experiment for South and South-West orientations
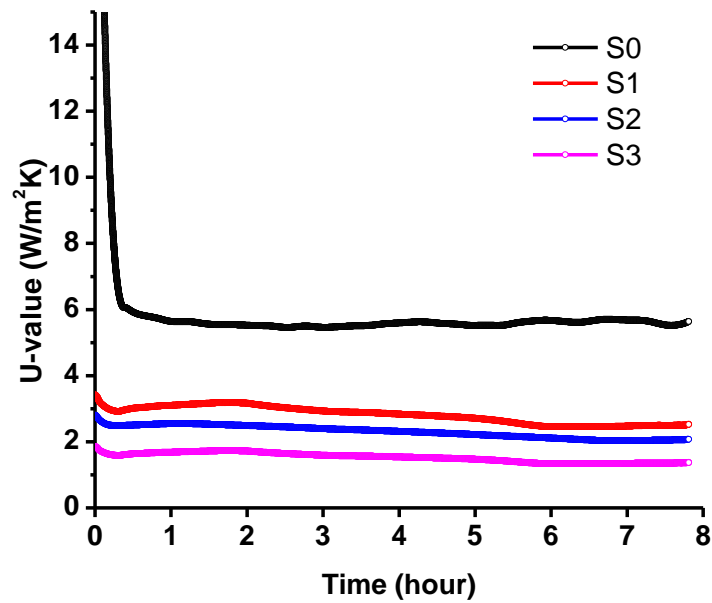

Figure 11.U-values from indoor experiment

4.3 Cooling Load

The measurement of cooling loads provides clear comparison figures of the thermal performance. AC energy consumption gives a clear representation of the cooling load inside the test cell. Cumulative energy consumption to maintain a set-point temperature of 23 ^{o}C was measured for the eight test cells in both outdoor orientations and results were represented in figure 12. For both orientations, the most consumption corresponds to the test cells at which clear glazing is fitted. The use of S_1, S_2 and S_3 glazing could induce reduction in cooling energy consumption of 7.7%, 14.7% and 23.2% in South-West direction and 4.4%, 8.2% and 11.9% in South direction compared to clear glazing.
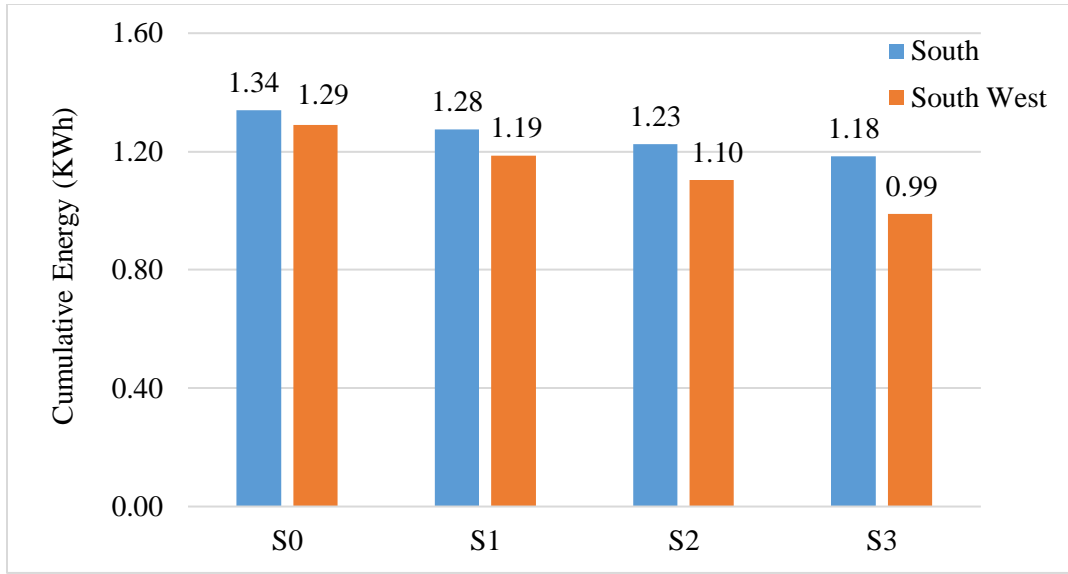
Figure 12. Cumulative Energy Consumption of AC unit

Cooling load results indicate that the use of S_3 PV glazing at South-West orientation is the best alternative of conventional single glazing as it leads to the most energy saving as well as most power generation among other glazing. However, S_3 glazing prohibits the transmission of visible solar radiation that represents the "daylight" leading to excessive use of artificial lighting. In addition, Among different indoor environment factors, daylight stands out to be of the most significance on occupants' health as it affects their mood, sleep quality and mental alertness (Shishegar & Boubekri, 2016) (Jamrozik et al., 2019). Thus, an optimum selection can be the use of S_1 or S_2 glazing that creates a compromise providing better optical conditions than S_3 and better tolerance to healthy environment while keeping the advantages of power generation and energy saving compared. Larger non-ventilated PV facades would provide more power generation and total energy saving for buildings. The U values of the different PV glazing studied and determined in this study are important parameters required for the calculation and estimation of the reduction of cooling load for buildings with these technologies. The design of energy-efficient buildings integrated with semi-transparent CdTe PV glazing necessities the knowledge of the results presented in this article to calculate the cooling load using the SHGC and U values illustrated in Figure 9 and Figure 10 respectively. The results of this paper fill a knowledge gap in the literature by these experimental results that help to quantify the energy savings for a building if this technology is used by the properties mentioned in the study. Other researchers can use this data to scall up their simulations to a big building and accurately estimate the total energy saving. Also, the thermal characterization of these samples can feed into industry and other researchers' databases to support other assessments for other types of buildings.

5. Conclusion

Thermal performance of three semi-transparent thin-film based CdTe glazing facades (S_1, S_2, S_3) was investigated by indoor and outdoor experimental tests for South and South West orientations under the conditions of the UK climate. The cells have visible transmissions of 24.83% for S_1,

18.66% for S_2 and 0.46% for S_3. The orientation was found to affect the diurnal variation of test cell temperatures and consequently the cooling energy. The U-values and SHGC for both orientations in outdoor experiment and indoor experiment showed very close values indicating constant thermal properties of the studied PV glazing regardless of the selected orientation. The indoor experiment showed steadier results of U-values due to variable outdoor ambient conditions. The lowest transparency PV glazing admitted an ability to reduce the solar heat gain by 96% while the higher transparency glazing S_1 and S_2 showed reduction of 72.3%, 80% respectively compared to the reference glazing. The measurement of cumulative cooling energy required by an AC unit prevailed the ability of S_1, S_2 and S_3 CdTe PV glazing to induce cooling reduction of 8%, 14.4% and 23.2% in South-West direction and 4.8%, 8.6% and 11.6% in South direction compared to single glazing. These results emphasized the advantages of CdTe PV glazing in hot and warm climates. For the sake of office-based non-ventilated Façade buildings, a compromise was targeted between power and daylight requirements for healthy indoor requirements and energy saving. The results can be utilized as reference for large scale buildings simulations to provide accurate estimates for the energy savings when this technology is used.

References

Alaaeddin, M. H., Sapuan, S. M., Zuhri, M. Y. M., Zainudin, E. S., & AL-Oqla, F. M. (2019). Photovoltaic applications: Status and manufacturing prospects. In *Renewable and Sustainable Energy Reviews* (Vol. 102, pp. 318–332). Elsevier Ltd. https://doi.org/10.1016/j.rser.2018.12.026

Allen, K., Connelly, K., Rutherford, P., & Wu, Y. (2017). Smart windows—Dynamic control of building energy performance. *Energy and Buildings*, *139*, 535–546. https://doi.org/10.1016/j.enbuild.2016.12.093

Alrashidi, H., Ghosh, A., Issa, W., Sellami, N., Mallick, T. K. T. K., & Sundaram, S. (2020). Thermal performance of semitransparent CdTe BIPV window at temperate climate. *Solar Energy*, *195*, 536–543. https://doi.org/10.1016/j.solener.2019.11.084

Alrashidi, H., Issa, W., Sellami, N., Ghosh, A., Mallick, T. K. T. K., & Sundaram, S. (2020). Performance assessment of cadmium telluride-based semi-transparent glazing for power saving in façade buildings. *Energy and Buildings*, *215*, 109585. https://doi.org/10.1016/j.enbuild.2019.109585

Alzoubi, H. H., & Al-Zoubi, A. H. (2010). Assessment of building façade performance in terms of daylighting and the associated energy consumption in architectural spaces: Vertical and horizontal shading devices for southern exposure facades. *Energy Conversion and Management*, *51*(8), 1592–1599. https://doi.org/10.1016/j.enconman.2009.08.039

Amelia, A. R., Irwan, Y. M., Leow, W. Z., Irwanto, M., Safwati, I., & Zhafarina, M. (2016). Investigation of the effect temperature on photovoltaic (PV) panel output performance. *International Journal on Advanced Science, Engineering and Information Technology*, *6*(5), 682–688. https://doi.org/10.18517/ijaseit.6.5.938

Barman, S., Chowdhury, A., Mathur, S., & Mathur, J. (2018). Assessment of the efficiency of window integrated CdTe based semi-transparent photovoltaic module. *Sustainable Cities and Society*, *37*, 250–262. https://doi.org/10.1016/J.SCS.2017.09.036

Bellia, L., De Falco, F., & Minichiello, F. (2013). Effects of solar shading devices on energy requirements of standalone office buildings for Italian climates. *Applied Thermal*

Engineering, *54*(1), 190–201. https://doi.org/10.1016/j.applthermaleng.2013.01.039

Biyik, E., Araz, M., Hepbasli, A., Shahrestani, M., Yao, R., Shao, L., Essah, E., Oliveira, A. C., del Caño, T., Rico, E., Lechón, J. L., Andrade, L., Mendes, A., & Atlı, Y. B. (2017). A key review of building integrated photovoltaic (BIPV) systems. *Engineering Science and Technology, an International Journal*, *20*(3), 833–858. https://doi.org/10.1016/j.jestch.2017.01.009

Chae, Y. T., Kim, J., Park, H., & Shin, B. (2014). Building energy performance evaluation of building integrated photovoltaic (BIPV) window with semi-transparent solar cells. *Applied Energy*, *129*, 217–227. https://doi.org/10.1016/j.apenergy.2014.04.106

Chen, F., Wittkopf, S. K., Khai Ng, P., & Du, H. (2012). Solar heat gain coefficient measurement of semi-transparent photovoltaic modules with indoor calorimetric hot box and solar simulator. *Energy and Buildings*, *53*, 74–84. https://doi.org/10.1016/J.ENBUILD.2012.06.005

Efficientwindows. (2018). *Solar Heat Gain Coefficient (SHGC) | Efficient Windows Collaborative*.

Favoino, F., Fiorito, F., Cannavale, A., Ranzi, G., & Overend, M. (2016). Optimal control and performance of photovoltachromic switchable glazing for building integration in temperate climates. *Applied Energy*, *178*, 943–961. https://doi.org/10.1016/j.apenergy.2016.06.107

Fung, T. Y. Y., & Yang, H. (2008). Study on thermal performance of semi-transparent building-integrated photovoltaic glazings. *Energy and Buildings*, *40*(3), 341–350. https://doi.org/10.1016/J.ENBUILD.2007.03.002

Ghosh, A., Norton, B., & Duffy, A. (2016). Measured thermal performance of a combined suspended particle switchable device evacuated glazing. *Applied Energy*, *169*, 469–480.

Jamrozik, A., Clements, N., Hasan, S. S., Zhao, J., Zhang, R., Campanella, C., Loftness, V., Porter, P., Ly, S., Wang, S., & Bauer, B. (2019). Access to daylight and view in an office improves cognitive performance and satisfaction and reduces eyestrain: A controlled crossover study. *Building and Environment*, *165*, 106379. https://doi.org/10.1016/j.buildenv.2019.106379

Fenestration of today and tomorrow: A state-of-the-art review and future research opportunities, 96 1 (2012) (testimony of BP Bjørn Petter Jelle, Andrew Hynd, Arild Gustavsen, Dariush Arasteh, Howdy Goudey, Robert Hart, & … D Arasteh -). https://doi.org/10.1016/j.solmat.2011.08.010

Khalifeeh, R., Alrashidi, H., Sellami, N., Mallick, T., & Issa, W. (2021). State-of-the-Art Review on the Energy Performance of Semi-Transparent Building Integrated Photovoltaic across a Range of Different Climatic and Environmental Conditions. *Energies 2021, Vol. 14, Page 3412*, *14*(12), 3412. https://doi.org/10.3390/EN14123412

Liao, W., & Xu, S. (2015). Energy performance comparison among see-through amorphous-silicon PV (photovoltaic) glazings and traditional glazings under different architectural conditions in China. *Energy*, *83*, 267–275. https://doi.org/10.1016/j.energy.2015.02.023

Mandalaki, M., Zervas, K., Tsoutsos, T., & Vazakas, A. (2012). Assessment of fixed shading devices with integrated PV for efficient energy use. *Solar Energy*, *86*(9), 2561–2575. https://doi.org/10.1016/j.solener.2012.05.026

McCandless, B. E., & Sites, J. R. (2011). Handbook of Photovoltaic Science and Engineering. In A. Luque & S. Hegedus (Eds.), *Handbook of Photovoltaic Science and Engineering* (Second). Wiley. https://doi.org/10.1002/9780470974704

Meillaud, F., Boccard, M., Bugnon, G., Despeisse, M., Hänni, S., Haug, F. J., Persoz, J., Schüttauf, J. W., Stuckelberger, M., & Ballif, C. (2015). Recent advances and remaining challenges in thin-film silicon photovoltaic technology. In *Materials Today* (Vol. 18, Issue 7, pp. 378–384). Elsevier B.V. https://doi.org/10.1016/j.mattod.2015.03.002

Noufi, R., & Zweibel, K. (2006). High-efficiency CdTe and CIGS thin-film solar cells: Highlights and challenges. *Conference Record of the 2006 IEEE 4th World Conference on Photovoltaic Energy Conversion, WCPEC-4*, *1*, 317–320. https://doi.org/10.1109/WCPEC.2006.279455

Olivieri, L., Caamaño-Martin, E., Olivieri, F., & Neila, J. (2014). Integral energy performance characterization of semi-transparent photovoltaic elements for building integration under real operation conditions. *Energy and Buildings*, *68*(PARTA), 280–291. https://doi.org/10.1016/j.enbuild.2013.09.035

Peng, J., Lu, L., Yang, H., & Ma, T. (2015). Comparative study of the thermal and power performances of a semi-transparent photovoltaic façade under different ventilation modes. *Applied Energy*, *138*, 572–583. https://doi.org/10.1016/j.apenergy.2014.10.003

Rezaei, S. D., Shannigrahi, S., & Ramakrishna, S. (2017). A review of conventional, advanced, and smart glazing technologies and materials for improving indoor environment. *Solar Energy Materials and Solar Cells*, *159*, 26–51. https://doi.org/10.1016/J.SOLMAT.2016.08.026

Romeo, N., Bosio, A., Menossi, D., Romeo, A., & Aramini, M. (2014). Last progress in CdTe/CdS thin film solar cell fabrication process. *Energy Procedia*, *57*, 65–72. https://doi.org/10.1016/j.egypro.2014.10.009

Samir, H., & Ali, N. A. (2017). Applying Building-integrated Photovoltaics (BIPV) in Existing Buildings, Opportunities and Constrains in Egypt. *Procedia Environmental Sciences*, *37*, 614–625. https://doi.org/10.1016/j.proenv.2017.03.048

Schultz, J. M., & Jensen, K. I. (2008). Evacuated aerogel glazings. *Vacuum*, *82*(7), 723–729. https://doi.org/10.1016/j.vacuum.2007.10.019

Shishegar, N., & Boubekri, M. (2016). Natural Light and Productivity: Analyzing the Impacts of Daylighting on Students' and Workers' Health and Alertness. *International Journal of Advances in Chemical Engineering and Biological Sciences*, *3*(1). https://doi.org/10.15242/ijacebs.ae0416104

Sidali, T., Bou, A., Coutancier, D., Chassaing, E., Theys, B., Barakel, D., Garuz, R., Thoulon, P. Y., & Lincot, D. (2018). Semi-transparent photovoltaic glazing based on electrodeposited CIGS solar cells on patterned molybdenum/glass substrates. *EPJ Photovoltaics*, *9*. https://doi.org/10.1051/epjpv/2017009

Skandalos, N., & Karamanis, D. (2016). Investigation of thermal performance of semi-transparent PV technologies. *Energy and Buildings*, *124*, 19–34. https://doi.org/10.1016/J.ENBUILD.2016.04.072

Skandalos, Nikolaos, & Karamanis, D. (2015). PV glazing technologies. In *Renewable and Sustainable Energy Reviews* (Vol. 49, pp. 306–322). Elsevier Ltd.

https://doi.org/10.1016/j.rser.2015.04.145

Smestad, G. P., Germer, T. A., Alrashidi, H., Fernández, E. F., Dey, S., Brahma, H., Sarmah, N., Ghosh, A., Sellami, N., Hassan, I. A. I., Desouky, M., Kasry, A., Pesala, B., Sundaram, S., Almonacid, F., Reddy, K. S., Mallick, T. K., & Micheli, L. (2020). Modelling photovoltaic soiling losses through optical characterization. *Scientific Reports*, *10*(1), 1–13. https://doi.org/10.1038/s41598-019-56868-z

Somasundaram, S., Chong, A., Wei, Z., & Thangavelu, S. R. (2020). Energy saving potential of low-e coating based retrofit double glazing for tropical climate. *Energy and Buildings*, *206*, 109570. https://doi.org/10.1016/j.enbuild.2019.109570

Song, J. H., An, Y. S., Kim, S. G., Lee, S. J., Yoon, J. H., & Choung, Y. K. (2008). Power output analysis of transparent thin-film module in building integrated photovoltaic system (BIPV). *Energy and Buildings*, *40*(11), 2067–2075. https://doi.org/10.1016/j.enbuild.2008.05.013

Sun, Y., Shanks, K., Baig, H., Zhang, W., Hao, X., Li, Y., He, B., Wilson, R., Liu, H., Sundaram, S., Zhang, J., Xie, L., Mallick, T., & Wu, Y. (2018). Integrated semi-transparent cadmium telluride photovoltaic glazing into windows: Energy and daylight performance for different architecture designs. *Applied Energy*, *231*, 972–984. https://doi.org/10.1016/J.APENERGY.2018.09.133

Waide, P. A., & Norton, B. (2003). Variation of insolation transmission with glazing plane position and sky conditions. *Journal of Solar Energy Engineering, Transactions of the ASME*, *125*(2), 182–189. https://doi.org/10.1115/1.1563630

Wang, M., Peng, J., Li, N., Yang, H., Wang, C., Li, X., & Lu, T. (2017). Comparison of energy performance between PV double skin facades and PV insulating glass units. *Applied Energy*, *194*, 148–160. https://doi.org/10.1016/J.APENERGY.2017.03.019

Yoon, J.-H., Song, J., & Lee, S.-J. (2011). Practical application of building integrated photovoltaic (BIPV) system using transparent amorphous silicon thin-film PV module. *Solar Energy*, *85*(5), 723–733. https://doi.org/10.1016/J.SOLENER.2010.12.026

Yun, G. Y., McEvoy, M., & Steemers, K. (2007). Design and overall energy performance of a ventilated photovoltaic façade. *Solar Energy*, *81*(3), 383–394. https://doi.org/10.1016/J.SOLENER.2006.06.016